Superpositions of *SU*(3) coherent states via a nonlinear evolution

2001 J. Phys. A: Math. Gen. 34 2051

(http://iopscience.iop.org/0305-4470/34/10/309)

INSTITUTE OF PHYSICS PUBLISHING JOURNAL OF PHYSICS A: MATHEMATICAL AND GENERAL

J. Phys. A: Math. Gen. **34** (2001) 2051–2062 www.iop.org/Journals/ja PII: S0305-4470(01)16131-7

Superpositions of $SU(3)$ coherent states via a nonlinear evolution

K Nemoto[1,3] **and B C Sanders**[2]

[1] Centre for Quantum Computer Technology, The University of Queensland, Queensland 4072, Australia
[2] Department of Physics, Macquarie University, Sydney, New South Wales 2109, Australia

Received 4 August 2000, in final form 22 January 2001

Abstract

We show that a nonlinear Hamiltonian evolution can transform an $SU(3)$ coherent state into a superposition of distinct $SU(3)$ coherent states, with a superposition of two $SU(2)$ coherent states presented as a special case. A phase-space representation is depicted by projecting the multi-dimensional Q-symbol for the state to a spherical subdomain of the coset space. We discuss realizations of this nonlinear evolution in the contexts of nonlinear optics and Bose–Einstein condensates.

PACS numbers: 0375F, 0375B, 0545

1. Introduction

The superposition principle in quantum physics implies that superpositions of probability amplitudes for classical-like states are possible, yet superpositions of quasi-classical quantum field states are not generally observed in practice. Such superposition states are especially interesting as they dramatically illustrate the quantum superposition principle by creating coherent superpositions of distinct states, with these distinct states behaving as classical physical states. Extensive theoretical and experimental studies have been directed towards understanding and obtaining superpositions of distinct quasi-classical states, often referred to as Schrödinger cat states [1, 2]. In general the interest has been in generating superpositions of Heisenberg–Weyl coherent states via a nonlinear Hamiltonian evolution [1, 3], where the Heisenberg–Weyl coherent states are the displaced harmonic-oscillator vacuum states.

Heisenberg–Weyl coherent states are relevant for studying the quantum–classical transition for the harmonic oscillator with one degree of freedom. The generalization to harmonic oscillators with two or more degrees of freedom leads to superpositions of product coherent states, or entangled coherent states, with a wealth of phenomena to be studied for such systems [4]. However, another generalization of superpositions of coherent states is possible by employing the generalized coherent states for general group actions [5]. Examples include superpositions of $SU(2)$ coherent states [6] and superpositions of $SU(1, 1)$ coherent states [7],

[3] Present address: School of Informatics, University of Wales, Bangor, UK.

as well as superpositions of multi-particle $SU(2)$ and $SU(1,1)$ coherent states [8]. Whereas the Heisenberg–Weyl group is the symmetry group for harmonic oscillators, $SU(2)$ is the symmetry group for spin precession, for two-channel interferometry and for the dynamics of ideal two-level atoms [5, 9–11], and $SU(1,1)$ is the symmetry group for the production of squeezed light and quantum interferometry with parametric up- and down-conversion [7, 11]. The generalized coherent states for such systems represent the quasi-classical states. For example the $SU(2)$ coherent states are also known as atomic coherent states and are analogous to classical electric dipoles [10]. Superpositions of these generalized coherent states in quantum systems are therefore of interest in studying counter-intuitive manifestations of the superposition principle.

The studies of superpositions of Heisenberg–Weyl, $SU(2)$ and $SU(1,1)$ coherent states are simplified by the fact that these are one-parameter groups, and the corresponding coset space is thus a locally two-dimensional manifold. For the Heisenberg–Weyl group, the manifold is the plane, for $SU(2)$ the Poincaré sphere and for $SU(1,1)$ the Lobachevsky plane. Here we generalize the studies of superpositions of coherent states to a two-parameter Lie group, namely $SU(3)$. The manifold for phase-space dynamics is the four-dimensional space isomorphic to the coset space $SU(3)/U(2)$. Working in a manifold which is greater than two dimensions presents problems in terms of visualizing the dynamics, which we resolve by projecting the dynamics to subdomains of spherical manifolds.

In order to generate superpositions of $SU(3)$ coherent states, we consider the three-dimensional nonlinear oscillator. Such a model can be realized by employing the three-boson realization of the $SU(3)$ generators and constructing the dynamics optically by employing passive optical devices and Kerr-type nonlinearities. Another physical system involves three interacting, independent Bose–Einstein condensates (BECs) [12]. In order to bring out the essential properties of superpositions of $SU(3)$ coherent states, we treat the dynamics as a closed system.

Superpositions of $SU(3)$ coherent states may be interesting from the perspective of weak force detection and accurate measurements. For example, weak force detection for two coupled, separated BECs employs a superposition of two extremal $SU(2)$ coherent states [13]. Superpositions of two extremal $SU(2)$ coherent states are valuable for related applications, such as precision measurement in particle interferometry [14]. Symmetries of $SU(3)$ coherent states may also prove to be valuable in the context of weak force detection for three coupled BECs or for three-channel particle interferometry, as examples.

We show that an initial $SU(3)$ coherent state in the nonlinear oscillator evolves to a superposition of $SU(3)$ coherent states. An analytical solution is provided which shows explicitly that a superposition of 16 $SU(3)$ coherent states occurs. The analytical solutions for the $SU(3)$ case are more complex and interesting than those for $SU(2)$, and we elaborate on the superposition of two $SU(2)$ coherent states as a special case. Graphical solutions are employed by using the Q-symbol (sometimes referred to as the Q-function) for the state and projecting to spherical subdomains. The graphical method provides an intuitive picture of the dynamics.

2. Three-dimensional nonlinear oscillator

The Hamiltonian for the three-dimensional nonlinear oscillator includes three pairs of annihilation and creation operators, designated by $\hat{c}_1, \hat{c}_1^\dagger, \hat{c}_2, \hat{c}_2^\dagger, \hat{c}_3, \hat{c}_3^\dagger$, with each pair $\{c_i, c_i^\dagger\}$ corresponding to one degree of freedom, or 'mode'. The usual boson commutation relation $[\hat{c}_k, \hat{c}_j^\dagger] = \delta_{kj}$ applies. We also define number operators as $\hat{n}_k = c_k^\dagger c_k$, and a total number

operator $\hat{N} = \sum_{k=1}^{3} \hat{n}_k$. We consider an isolated system; hence, total energy and total particle number are conserved. In particular we are interested in the simplest system with energy and number conservation which will allow an $SU(3)$ coherent state to evolve into a superposition of $SU(3)$ coherent states. Such a Hamiltonian is given by

$$H = \omega \sum_{k=1}^{3} \hat{n}_k + \chi_1(t) \sum_{k=1}^{3} \hat{n}_k^{\dagger}(\hat{n}_k - 1) + \chi_2(t) \sum_{\substack{j,k=1 \\ j \neq k}}^{3} \hat{n}_k \hat{n}_j + \sum_{\substack{j,k=1 \\ j \neq k}}^{3} \Omega_{jk}(t) c_j^{\dagger} c_k \qquad (1)$$

with $\Omega_{jk}(t) = \Omega_{kj}^{*}(t)$. In this model, the coupling constant χ_1 corresponds to the strength of the self-modulation term, and χ_2 is the strength of the cross-modulation term. The time-dependent quantities χ_i are assumed to be controllable as well as the time-dependent coupling strengths Ω_{jk} that are responsible for linear coupling between modes. For the case where each mode corresponds to bosons in a particular spatial region, the terms χ_i quantify the nonlinear interactions, and Ω_{jk} quantify the strength of (linear) quantum tunnelling of bosons between modes. For $\chi_i = 0$, with $i = 1, 2$, the Hamiltonian (1) is a linear combination of $su(3)$ generators, and thus the evolution is linear.

The Hamiltonian (1) corresponds to two potential physical realizations, the first being a nonlinear optical four-wave mixing medium, that is a medium with a $\chi^{(3)}$ nonlinearity. In four-wave mixing, the three boson operators c_k correspond to single-mode fields interacting in the medium, and the coefficients χ_i, $i \in \{1, 2\}$ are obtained by judiciously constructing the $\chi^{(3)}$ tensor coefficients.

A second realization arises in the context of interacting BECs with a small number of particles [12, 15], which is of interest for some condensates [16]. The three boson operators correspond to localized BEC modes with some overlap between the modes (in contrast to the case considered in [12], which assumes a negligible overlap). The localized modes are centred around the three minima of a three-dimensional trapping potential for the BEC. The nonlinear interactions arise due to atomic collisions and conserve boson number. The coefficients for the nonlinear interactions are χ_1, for self interactions, and χ_2, for intermodal collisions. These parameters depend on the s-wave scattering length for the condensate and its density as well as the degree of overlap between modes for χ_2. These coefficients of nonlinear dynamical terms are time dependent: the scattering length can be varied by applying an external magnetic field to exploit a Feshbach resonance in the collisions between the atoms [17].

The time-varying linear quantum tunnelling terms for the BEC, with coefficients Ω_{jk}, may be varied by modifying the optical potential barrier between minima of the trapping potential. The terms are left on for a short time to produce the desired $SU(3)$ coherent state and then shut off. Of course they are not completely eliminated as some overlap is needed for the cross-mode collisions (with coefficient χ_2) to take place. It is important that the collision terms be strong enough to be non-negligible even when linear quantum tunnelling may be ignored. Tuning the scattering length is advantageous to ensure that the intermodal collision term is sufficiently strong. Although χ_2 might be weak, our subsequent analysis is valid for any choice of χ_2.

A typical initial condition could be N bosons in one region or mode. Allowing the system to evolve under the Hamiltonian (1) with $\chi_i = 0$ causes the system to evolve linearly, via coherent quantum tunnelling, to a Perelomov $SU(3)$ coherent state [5]. As a special case, relevant to weak-force detection [13] and particle interferometry [14], extremal coherent states are states which are mapped to zero under a ladder operator. For example, the $SU(2)$ coherent state $|j\ j\rangle$ is annihilated by the specified raising operator J_+, and the state $|j\ -j\rangle$ is annihilated by the specified lowering operator J_-. These two states are extremal, and a superposition of these two extremal states would be $(|j\ j\rangle + |j\ -j\rangle)/\sqrt{2}$. Extremal $SU(3)$ coherent states are states which can be annihilated by the $su(3)$ ladder operators.

From conservation of the total number N of bosons, the Hamiltonian may be rewritten in terms of the $SU(3)$ generators and the total number N is the irreducible representation (irrep) parameter. The eight generators of $SU(3)$ may be defined as the two Cartan operators

$$X_1 = \hat{c}_1^\dagger \hat{c}_1 - \hat{c}_2^\dagger \hat{c}_2 \tag{2a}$$

$$X_2 = \tfrac{1}{3}(\hat{c}_1^\dagger \hat{c}_1 + \hat{c}_2^\dagger \hat{c}_2 - 2\hat{c}_3^\dagger \hat{c}_3^\dagger) \tag{2b}$$

and the six generators

$$Y_k = \mathrm{i}(\hat{c}_k^\dagger \hat{c}_j - \hat{c}_j^\dagger \hat{c}_k) \tag{3a}$$

$$Z_k = \hat{c}_k^\dagger \hat{c}_j + \hat{c}_j^\dagger \hat{c}_k \tag{3b}$$

where $k = 1, 2, 3$ and $j = k \bmod 3 + 1$. The raising operators and lowering operators are defined as

$$J_+^k = \hat{c}_k^\dagger \hat{c}_j \qquad (k < j) \tag{4a}$$

$$J_-^k = \hat{c}_k^\dagger \hat{c}_j \qquad (k > j) \tag{4b}$$

or, alternatively, for $k < j$

$$J_+^k = \tfrac{1}{2}(Z_k - \mathrm{i}Y_k) \tag{5a}$$

$$J_-^k = \tfrac{1}{2}(Z_k + \mathrm{i}Y_k) \tag{5b}$$

in terms of $SU(3)$ generators.

The term involving the irrep parameter N can be removed by moving to a rotating picture. Furthermore, by assuming that the initial $SU(3)$ coherent state has been generated from the evolution (1), with large linear quantum tunnelling and negligible contributions from nonlinear evolution, the optical potential barrier between trapping potential minima is increased to reduce the linear tunnelling. At the same time, the nonlinear coefficients must be reasonably large compared to the coefficient for linear tunnelling, perhaps by employing an external magnetic field to exploit a Feshbach resonance, as discussed above. For large nonlinearities and small linear quantum tunnelling terms, the Hamiltonian (1) can be approximated by

$$H = \frac{\chi}{2}(X_1^2 + 3X_2^2) \tag{6}$$

with $\chi = \chi_1 - \chi_2$. The Hamiltonian is a sum of quadratic forms of Cartan operators which commute, and this property will be useful in later calculations.

3. Coherent states

3.1. $SU(2)$ coherent states

In order to introduce the $SU(3)$ coherent states, it is useful to review the $SU(2)$ coherent states and to use this knowledge to generalize to $SU(3)$ coherent states. $SU(2)$ coherent states and their methods were first developed as atomic coherent states [9, 10] to treat atomic systems. On the other hand, coherent states for Lie groups were defined by Perelomov [5] as an orbit generated by group action on a reference state, which is usually the highest- (or lowest-) weight state. For compact groups, the simplest nontrivial case is $SU(2)$, which can be parametrized by three real parameters $\{\theta, \varphi_1, \varphi_2\}$. The lowest-order faithful representation of an arbitrary $g \in SU(2)$ is as a 2×2 matrix

$$g(\varphi_1, \theta, \varphi_2) = \begin{pmatrix} \mathrm{e}^{\mathrm{i}\varphi_1} \cos\theta & \mathrm{e}^{\mathrm{i}\varphi_2} \sin\theta \\ -\mathrm{e}^{-\mathrm{i}\varphi_2} \sin\theta & \mathrm{e}^{-\mathrm{i}\varphi_1} \cos\theta \end{pmatrix}. \tag{7}$$

As $SU(2) \subset SU(3)$, the three generators of $SU(2)$ can be obtained from (2*a*), (2*b*), (3*a*) and (3*b*). For example, the subgroup $SU(2)_{12}$ is generated by $\{X_1, Y_1, Z_1\}$. The Casimir invariant is $J^2 = X_1^2 + Y_1^2 + Z_1^2$ with eigenvalue $j(j+1)$. The 2×2 representation corresponds to $j = 1/2$. The weight basis corresponds to $|jm\rangle$ with $J_z|jm\rangle = m|jm\rangle$. The highest-weight state is $|jj\rangle$ for which $J_+|jj\rangle = 0$.

The $SU(2)$ coherent state, for fixed j, is given by

$$|\theta, \varphi\rangle = \exp\left[-\frac{\theta}{2}(J_+^1 \mathrm{e}^{-\mathrm{i}\varphi} - J_-^1 \mathrm{e}^{\mathrm{i}\varphi})\right] |j\ j\rangle. \tag{8}$$

The coherent state can be represented geometrically on the Poincaré sphere, which is isomorphic to the coset space $SU(2)/U(1)$.

3.2. $SU(3)$ *coherent states*

The $SU(3)$ coherent states may be formulated as a generalization of the $SU(2)$ coherent states [18, 19], and are obtained by the action of $SU(3)$ on the highest-weight state. In order to obtain the $SU(3)$ coherent states, it is convenient to employ the decomposition of $SU(3)$ in [20], whereby the $SU(3)$ operator is decomposed into a combination of $SU(2)$ operators. The decomposition allows us to parametrize an arbitrary element g in the 3×3 matrix representation as

$$g = \begin{pmatrix} 1 & 0 & 0 \\ 0 & & \\ 0 & & V \end{pmatrix} \begin{pmatrix} \mathrm{e}^{\mathrm{i}\varphi}\cos\theta & -\sin\theta & 0 \\ \sin\theta & \mathrm{e}^{-\mathrm{i}\varphi}\cos\theta & 0 \\ 0 & 0 & 1 \end{pmatrix} \begin{pmatrix} 1 & 0 & 0 \\ 0 & & \\ 0 & & W \end{pmatrix} \tag{9}$$

where $V(\varphi_1, \xi, \varphi_2)$ and $W(\varphi_3, \zeta, \varphi_4)$ are 2×2 matrices representing elements of $SU(2)_{23}$. The middle matrix on the right-hand side of equation (9) is an element of $SU(2)_{12}$.

The $SU(3)$ generators of equations (2*a*), (2*b*) and (3*a*), (3*b*) are presented as a three-boson realization. It is convenient to employ the basis states, which are eigenstates of the $SU(3)$ Casimir operators and of the two elements of the Cartan subalgebra (2*a*), (2*b*). The basis state can be labelled by the three numbers n_1, n_2 and n_3, which satisfy

$$\hat{n}_k|n_1, n_2, n_3\rangle = n_k|n_1, n_2, n_3\rangle \qquad \text{for} \quad k \in \{1, 2, 3\}. \tag{10}$$

As any action of the raising operators on the state $|N, 0, 0\rangle$ annihilates it, the state $|N, 0, 0\rangle$ is a highest-weight state. Coherent states are obtained by $SU(3)$ action on this highest-weight state.

Taking the highest-weight state $|N, 0, 0\rangle$ as the reference state, the action of equation (9) on the highest-weight state gives an explicit form of coherent states. The factorization (9) ensures that the matrix on the furthest right leaves the highest-weight state invariant, and only the two other matrices are important in determining the coherent state. The highest-weight state is thus invariant under $SU(2)_{23}$; hence the coherent states are parametrized on the coset space $SU(3)/SU(2)$. In fact the $SU(3)$ coherent states can be parametrized on the coset space $SU(3)/U(2)$ by eliminating an arbitrary phase, but the following calculations are easier if we retain the phase. In calculations of the Q-symbol for the state, this phase is not important.

The coherent states can be generated as

$$|\xi, \theta, \varphi, \varphi_1, \varphi_2\rangle = g(\varphi_1, \xi, \varphi_2, \varphi, \theta, \varphi_3, \zeta, \varphi_4)|N, 0, 0\rangle \tag{11}$$

which can be expressed as

$$|\xi, \theta, \varphi, \varphi_1, \varphi_2\rangle = \sum_{j_1=0}^{N} \mathrm{e}^{\mathrm{i}\varphi(N-j_1)} \sin^{j_1}(\theta) \cos^{(N-j_1)}(\theta) \binom{N}{j_1}^{1/2}$$

$$\times \sum_{j_2=0}^{j_1} \mathrm{e}^{\mathrm{i}j_2\varphi_2}\mathrm{e}^{\mathrm{i}\varphi_1(j_1-j_2)} \sin^{j_2}(\xi)\cos^{(j_1-j_2)}(\xi)\begin{pmatrix} j_1 \\ j_2 \end{pmatrix}^{1/2} |N-j_1, j_1-j_2, j_2\rangle. \tag{12}$$

This parametrization of the $SU(3)$ coherent state includes an arbitrary phase.

4. Quantum dynamics of the system

4.1. Analytical solutions

Let the initial state $|\psi(0)\rangle$ be an arbitrary $SU(3)$ coherent state. The state $|\psi(t)\rangle$ for arbitrary time t may thus be given as

$$\begin{aligned}|\psi(t)\rangle = \sum_{j_1=0}^{N} \mathrm{e}^{\mathrm{i}\varphi(N-j_1)} \sin^{j_1}(\theta)\cos^{(N-j_1)}(\theta)\begin{pmatrix} N \\ j_1 \end{pmatrix}^{1/2} \sum_{j_2=0}^{j_1} \mathrm{e}^{\mathrm{i}j_2\varphi_2}\mathrm{e}^{\mathrm{i}\varphi_1(j_1-j_2)} \sin^{j_2}(\xi) \\ \times \cos^{(j_1-j_2)}(\xi)\begin{pmatrix} j_1 \\ j_2 \end{pmatrix}^{1/2} \exp\left[-2\mathrm{i}\chi t(N^2/3 + j_1^2 + j_2^2 - j_1(N+j_2))\right] \\ \times |N-j_1, j_1-j_2, j_2\rangle\end{aligned} \tag{13}$$

under the Hamiltonian evolution (6). The time-dependent element of equation (13) exhibits the periodic evolution of the state and suggests that the state evolves into superposition states periodically, by analogy with the $SU(2)$ coherent state superposition case [6], but with additional complexity due to the greater number of parameters and the higher dimension of the group manifold.

From equation (13), we observe that the recurrence time, for which the state evolves cyclically back into the original state, is given by $\tau \equiv \pi/\chi$ for all values of the irrep parameter N. At half the recurrence time, $\tau/2 = \pi/2\chi$, the state evolves into the superposition

$$\begin{aligned}|\psi(\tau/2)\rangle = \tfrac{1}{2}\mathrm{e}^{-\mathrm{i}\pi N^2/3}[-|\xi,\theta,\varphi,\varphi_1,\varphi_2\rangle + |\xi,\theta,\varphi,\varphi_1+\pi,\varphi_2\rangle + |\xi,\theta,\varphi,\varphi_1,\varphi_2\rangle \\ +|\xi,\theta,\varphi,\varphi_1+\pi,\varphi_2+\pi\rangle]\end{aligned} \tag{14}$$

for even N, or

$$\begin{aligned}|\psi(\tau/2)\rangle = \tfrac{1}{2}\mathrm{e}^{-\mathrm{i}\pi N^2/3}[|\xi,\theta,\varphi,\varphi_1,\varphi_2\rangle + |\xi,\theta,\varphi+\pi,\varphi_1,\varphi_2\rangle + |\xi,\theta,\varphi,\varphi_1+\pi,\varphi_2\rangle \\ +|\xi,\theta,\varphi,\varphi_1,\varphi_2+\pi\rangle]\end{aligned} \tag{15}$$

for odd N. At one-quarter of the recurrence time $\tau/4$, the state evolves into a superposition state with the exact form depending on the total number N. There are four types of superposition state at $\tau/4$, classified by the quantity N mod 4. The four types are given as the following.

(1) If $N = 4n$, for n an integer,

$$\begin{aligned}|\psi(\tau/4)\rangle = \tfrac{1}{4}\mathrm{e}^{-\mathrm{i}\pi N^2/6}\Bigg[|\xi,\theta,\varphi,\varphi_1,\varphi_2\rangle + |\xi,\theta,\varphi,\varphi_1+\pi,\varphi_2\rangle + |\xi,\theta,\varphi,\varphi_1,\varphi_2+\pi\rangle \\ +|\xi,\theta,\varphi,\varphi_1+\pi,\varphi_2+\pi\rangle \\ +\mathrm{i}\Bigg(-\left|\xi,\theta,\varphi,\varphi_1,\varphi_2-\frac{\pi}{2}\right\rangle - \left|\xi,\theta,\varphi,\varphi_1,\varphi_2+\frac{\pi}{2}\right\rangle \\ +\left|\xi,\theta,\varphi,\varphi_1+\frac{\pi}{2},\varphi_2-\frac{\pi}{2}\right\rangle - \left|\xi,\theta,\varphi,\varphi_1+\frac{\pi}{2},\varphi_2+\frac{\pi}{2}\right\rangle \\ +\left|\xi,\theta,\varphi,\varphi_1+\frac{\pi}{2},\varphi_2+\pi\right\rangle - \left|\xi,\theta,\varphi,\varphi_1+\frac{\pi}{2},\varphi_2\right\rangle\end{aligned}$$

$$+\left|\xi,\theta,\varphi,\varphi_1+\pi,\varphi_2-\frac{\pi}{2}\right\rangle+\left|\xi,\theta,\varphi,\varphi_1+\pi,\varphi_2+\frac{\pi}{2}\right\rangle$$
$$-\left|\xi,\theta,\varphi,\varphi_1-\frac{\pi}{2},\varphi_2-\frac{\pi}{2}\right\rangle+\left|\xi,\theta,\varphi,\varphi_1-\frac{\pi}{2},\varphi_2+\frac{\pi}{2}\right\rangle$$
$$-\left|\xi,\theta,\varphi,\varphi_1-\frac{\pi}{2},\varphi_2\right\rangle+\left|\xi,\theta,\varphi,\varphi_1-\frac{\pi}{2},\varphi_2+\pi\right\rangle\Big)\Big]. \tag{16}$$

(2) If $N=4n+1$,

$$|\psi(\pi/4\chi)\rangle=\frac{1}{4}\mathrm{e}^{-\mathrm{i}\pi N^2/6}\Big[\left|\xi,\theta,\varphi,\varphi_1+\frac{\pi}{2},\varphi_2+\frac{\pi}{2}\right\rangle+\left|\xi,\theta,\varphi,\varphi_1-\frac{\pi}{2},\varphi_2+\frac{\pi}{2}\right\rangle$$
$$+\left|\xi,\theta,\varphi,\varphi_1+\frac{\pi}{2},\varphi_2-\frac{\pi}{2}\right\rangle+\left|\xi,\theta,\varphi,\varphi_1-\frac{\pi}{2},\varphi_2-\frac{\pi}{2}\right\rangle$$
$$+\mathrm{i}\Big(-\left|\xi,\theta,\varphi,\varphi_1+\frac{\pi}{2},\varphi_2\right\rangle-\left|\xi,\theta,\varphi,\varphi_1+\frac{\pi}{2},\varphi_2+\pi\right\rangle$$
$$+\left|\xi,\theta,\varphi,\varphi_1+\pi,\varphi_2\right\rangle-\left|\xi,\theta,\varphi,\varphi_1+\pi,\varphi_2+\pi\right\rangle$$
$$+\left|\xi,\theta,\varphi,\varphi_1+\pi,\varphi_2-\frac{\pi}{2}\right\rangle-\left|\xi,\theta,\varphi,\varphi_1+\pi,\varphi_2+\frac{\pi}{2}\right\rangle$$
$$+\left|\xi,\theta,\varphi,\varphi_1-\frac{\pi}{2},\varphi_2\right\rangle+\left|\xi,\theta,\varphi,\varphi_1-\frac{\pi}{2},\varphi_2+\pi\right\rangle$$
$$-|\xi,\theta,\varphi,\varphi_1,\varphi_2\rangle+|\xi,\theta,\varphi,\varphi_1,\varphi_2+\pi\rangle-\left|\xi,\theta,\varphi,\varphi_1,\varphi_2+\frac{\pi}{2}\right\rangle$$
$$+\left|\xi,\theta,\varphi,\varphi_1,\varphi_2-\frac{\pi}{2}\right\rangle\Big)\Big]. \tag{17}$$

(3) If $N=4n+2$,

$$|\psi(\tau/4)\rangle=\tfrac{1}{4}\mathrm{e}^{-\mathrm{i}\pi N^2/6}\Big[|\xi,\theta,\varphi,\varphi_1,\varphi_2\rangle+|\xi,\theta,\varphi,\varphi_1+\pi,\varphi_2\rangle+|\xi,\theta,\varphi,\varphi_1,\varphi_2+\pi\rangle$$
$$+|\xi,\theta,\varphi,\varphi_1+\pi,\varphi_2+\pi\rangle$$
$$+\mathrm{i}\Big(-\left|\xi,\theta,\varphi,\varphi_1+\pi,\varphi_2+\frac{\pi}{2}\right\rangle-\left|\xi,\theta,\varphi,\varphi_1+\pi,\varphi_2-\frac{\pi}{2}\right\rangle$$
$$+\left|\xi,\theta,\varphi,\varphi_1-\frac{\pi}{2},\varphi_2+\frac{\pi}{2}\right\rangle-\left|\xi,\theta,\varphi,\varphi_1-\frac{\pi}{2},\varphi_2-\frac{\pi}{2}\right\rangle$$
$$+\left|\xi,\theta,\varphi,\varphi_1-\frac{\pi}{2},\varphi_2\right\rangle-\left|\xi,\theta,\varphi,\varphi_1-\frac{\pi}{2},\varphi_2+\pi\right\rangle$$
$$+\left|\xi,\theta,\varphi,\varphi_1,\varphi_2+\frac{\pi}{2}\right\rangle+\left|\xi,\theta,\varphi,\varphi_1,\varphi_2-\frac{\pi}{2}\right\rangle$$
$$-\left|\xi,\theta,\varphi,\varphi_1+\frac{\pi}{2},\varphi_2+\frac{\pi}{2}\right\rangle+\left|\xi,\theta,\varphi,\varphi_1+\frac{\pi}{2},\varphi_2-\frac{\pi}{2}\right\rangle$$
$$-\left|\xi,\theta,\varphi,\varphi_1+\frac{\pi}{2},\varphi_2+\pi\right\rangle+\left|\xi,\theta,\varphi,\varphi_1+\frac{\pi}{2},\varphi_2\right\rangle\Big)\Big]. \tag{18}$$

(4) If $N=4n+3$,

$$|\psi(\tau/4)\rangle=\frac{1}{4}\mathrm{e}^{-\mathrm{i}\pi N^2/6}\Big[\left|\xi,\theta,\varphi,\varphi_1-\frac{\pi}{2},\varphi_2-\frac{\pi}{2}\right\rangle+\left|\xi,\theta,\varphi,\varphi_1+\frac{\pi}{2},\varphi_2-\frac{\pi}{2}\right\rangle$$

$$+\left|\xi,\theta,\varphi,\varphi_1-\frac{\pi}{2},\varphi_2+\frac{\pi}{2}\right\rangle+\left|\xi,\theta,\varphi,\varphi_1+\frac{\pi}{2},\varphi_2+\frac{\pi}{2}\right\rangle$$
$$+\mathrm{i}\Bigg(-\left|\xi,\theta,\varphi,\varphi_1-\frac{\pi}{2},\varphi_2+\pi\right\rangle-\left|\xi,\theta,\varphi,\varphi_1-\frac{\pi}{2},\varphi_2\right\rangle$$
$$+|\xi,\theta,\varphi,\varphi_1,\varphi_2+\pi\rangle-|\xi,\theta,\varphi,\varphi_1,\varphi_2\rangle$$
$$+\left|\xi,\theta,\varphi,\varphi_1,\varphi_2+\frac{\pi}{2}\right\rangle-\left|\xi,\theta,\varphi,\varphi_1,\varphi_2-\frac{\pi}{2}\right\rangle$$
$$+\left|\xi,\theta,\varphi,\varphi_1+\frac{\pi}{2},\varphi_2+\pi\right\rangle+\left|\xi,\theta,\varphi,\varphi_1+\frac{\pi}{2},\varphi_2\right\rangle$$
$$-|\xi,\theta,\varphi,\varphi_1+\pi,\varphi_2+\pi\rangle+|\xi,\theta,\varphi,\varphi_1+\pi,\varphi_2\rangle$$
$$-\left|\xi,\theta,\varphi,\varphi_1+\pi,\varphi_2-\frac{\pi}{2}\right\rangle+\left|\xi,\theta,\varphi,\varphi_1+\pi,\varphi_2+\frac{\pi}{2}\right\rangle\Bigg)\Bigg]. \tag{19}$$

4.2. The Q-symbol

In the previous section we obtained analytical expressions of $|\psi(t)\rangle$ for two particular time values, $\tau/2$ and $\tau/4$. More generally however we can obtain the state analytically for all values of t. The density matrix $\rho(t)$ for the system may be written in terms of the pure state $|\psi(t)\rangle$ as

$$\rho(t)=|\psi(t)\rangle\langle\psi(t)|. \tag{20}$$

The Q-symbol for this state is given by [5]

$$Q(t)=\langle\xi,\theta,\varphi,\varphi_1,\varphi_2|\rho(t)|\xi,\theta,\varphi,\varphi_1,\varphi_2\rangle. \tag{21}$$

The arbitrary phase disappears in the calculation of $Q(t)$. It is thus convenient to employ the two relative phases $\phi_1=\varphi_1-\varphi$ and $\phi_2=\varphi_2-\varphi_1$. The Q-symbol for the state may thus be expressed as

$$Q(\xi,\theta,\phi_1,\phi_2:\xi(0),\theta(0),\phi_1(0),\phi_2(0);t)=\left|\sum_{j_1=0}^{N}\sum_{j_2=0}^{j_1}S^N_{j_1,j_2}(\xi,\theta,\phi_1,\phi_2;t)\right|^2 \tag{22}$$

where

$$S^N_{j_1,j_2}=\mathrm{e}^{-\mathrm{i}j_1(\phi_1-\phi_1(0))}(\sin\theta\sin\theta(0))^{j_1}(\cos\theta\cos\theta(0))^{N-j_1}\binom{N}{j_1}$$
$$\times\mathrm{e}^{-\mathrm{i}j_1(\phi_2-\phi_2(0))}(\sin\xi\sin\xi(0))^{j_1}(\cos\xi\cos\xi(0))^{N-j_1}\binom{j_1}{j_2}$$
$$\times\mathrm{e}^{-2\mathrm{i}\chi t(j_1^2+j_2^2-j(N+j_2))}. \tag{23}$$

The Q-symbol depends on four periodic parameters, and therefore a plot of the Q-symbol would need to be embedded in five-dimensional space to be viewed. However, in order to view the plot we need to reduce the number of dimensions required for plotting the function. A simple way to plot the Q-symbol is to fix one parameter, for example by setting $\theta=\pi/2$. This corresponds to a *slice* of the Q-symbol, and the choice of where to slice depends on the features to be emphasized in the plot. A slice is a standard means for representing multi-dimensional figures; animation can be used, for example, to present the figure by 'travelling' through a sequence of slices. We will present an example in the following subsection.

4.3. An example

The nonlinear $SU(2)$ oscillator generates superposition states from an initial $SU(2)$ coherent state and can generate a superposition of two distinct $SU(2)$ coherent states at a half of its

recurrence time [6]. This superposition of two distinct $SU(2)$ coherent states results in two major peaks arising in the plot of the Q-symbol for the superposition state. Interference fringes midway between the two peaks arise due to the coherence properties of the superposition. These interference fringes can be clearly seen as dimples in a plot of the logarithm of the Q-symbol [21].

The superposition states we have seen in equations (16)–(19) arise from the nonlinearity of the $SU(3)$ system. In this subsection, we wish to observe a manifestation of such a superposition by plotting the Q-symbol for the state. As discussed in the previous subsection, we can reduce the dimension of the parameter space to two by obtaining a slice of the Q-symbol for the state. We consider an $SU(3)$ coherent state which is also an $SU(2)_{23}$ coherent state. This restriction to $SU(2)_{23}$ coherent states ensures that only a subset of the Q-symbol is explored, with this subset being a slice which can be plotted on the Poincaré sphere corresponding to the $SU(2)_{23}/U(1)$ coset space. An initial $SU(2)_{23}$ coherent state can be written as

$$\begin{aligned}|\psi(0)\rangle &= |\xi(0), \pi/2, \phi_1(0), \phi_2(0)\rangle \\ &= \mathrm{e}^{-\mathrm{i}\phi_1(0)N}\sum_{j_2=0}^{N}\mathrm{e}^{\mathrm{i}\phi_2(0)j_2}\sin^{j_2}(\xi(0))\cos^{(N-j_2)}(\xi(0))\binom{N}{j_2}^{1/2}|0, N-j_2, j_2\rangle. \quad (24)\end{aligned}$$

A state in the $SU(2)_{23}$ subsystem stays in this subsystem under time evolution, so the factor of ϕ_1 becomes an arbitrary phase and disappears in the calculation of the Q-symbol. We now employ the notation $\tilde{Q}$ to refer to a slice of the Q-symbol. In this notation, the reduced Q-symbol, with the initial condition (24), is given by

$$\begin{aligned}\tilde{Q}(\theta, \xi, \phi_2; t) &= \langle \xi, \theta, \phi_1, \phi_2|\rho(t)|\xi, \theta, \phi_1, \phi_2\rangle \\ &= \sin^{2N}(\theta)\sum_{p=0}^{N}\sum_{q=0}^{N}\mathrm{e}^{-\mathrm{i}(p-q)(\phi_2-\phi_2(0))}(\sin(\xi)\sin(\xi(0)))^{p+q} \\ &\quad\times(\cos(\xi)\cos(\xi(0)))^{(2N-(p+q))} \\ &\quad\times\binom{N}{p}\binom{N}{q}\exp[-2\mathrm{i}\chi t(p-q)(p-q-N)]. \quad (25)\end{aligned}$$

The (θ)-component of the Q-symbol is time independent with a fixed weighting of $\sin^{2N}(\theta)$. The optimal slice for observing the Q-symbol in the reduced ξ–ϕ_2 space is thus obtained by setting $\theta = \pi/2$.

With the initial condition $\xi(0) = \pi/4$, $\phi_2(0) = 0$, $\tilde{Q}$ is simplified to

$$\begin{aligned}\tilde{Q}(\xi, \phi_2 : t) &= 2^{-N}\sum_{p=0}^{N}\sum_{q=0}^{N}\mathrm{e}^{-\mathrm{i}(p-q)\phi_2}\binom{N}{p}\binom{N}{q}\sin^{p+q}(\xi)\cos^{(2N-(p+q))}(\xi) \\ &\quad\times\exp[-2\mathrm{i}\chi t(p-q)(p+q-N)] \quad (26)\end{aligned}$$

and is numerically represented in figures 1 and 2. The time-dependent term in equation (26) implies that the time evolution of the state is distinguishable in terms of the total number N. The product $(p-q)(p+q-N)$ is even for any p and q if N is odd, whereas it is not true for any even total number N. The recurrence time of the time evolution with an odd total number N is a half of the recurrence time with an even total number. We solve this evolution numerically and plot $\tilde{Q}$ as it evolves for two values of the total number, $N = 9, 10$. Figure 1 shows the time evolution of $\tilde{Q}$ for the state for even number $N = 10$; in contrast, figure 2 depicts the time evolution of $\tilde{Q}$ for the state for odd number $N = 9$.

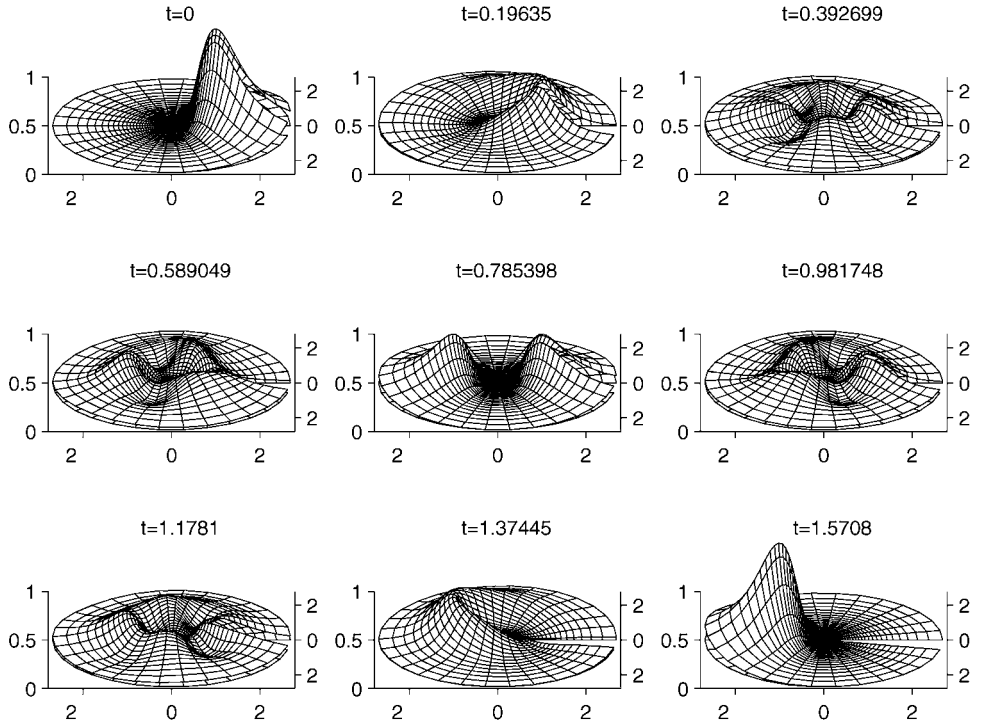

Figure 1. $\tilde{Q}(\xi, \phi_2)$ is plotted at a certain time t with the use of stereographical mapping. The origin corresponds to the north pole of the spherical subdomain (ξ, ϕ_2). Time flows from the top left figure at $t = 0$ to the bottom right figure at $t = \tau/2$. The recurrence time is twice as long as the odd-number case in figure 2.

5. Conclusions

We have investigated the formation of superpositions of $SU(3)$ coherent states via a nonlinear Hamiltonian evolution. This evolution could be realized in terms of four-wave mixing in nonlinear optics or in terms of a nonlinear interaction between three independent modes of a BEC with non-negligible nonlinear interactions between the separate, but overlapping, modes. The linear quantum tunnelling term is allowed to vary independently of the nonlinear (collision) terms, and linear quantum tunnelling is used to prepare the $SU(3)$ coherent state for N bosons in the three modes. Then this $SU(3)$ coherent state undergoes a nonlinear evolution into a superposition of $SU(3)$ coherent states.

We have obtained explicit expressions for the superposition of coherent states at one-half and one-quarter the recurrence time for this periodic evolution. Whereas superpositions of pairs of coherent states are obtained for half the recurrence time for Heisenberg–Weyl, $SU(2)$ and $SU(1, 1)$ systems, the higher dimension of $SU(3)$ dynamics leads to much more complex and interesting superpositions even at half the recurrence time. The nature of the superposition depends on the quantity N mod 4, with N being the total quantum number. The state at some time t can be represented by the use of a Q-symbol representation. However, the multi-dimensional domain of the Q-symbol makes the visualization of this function challenging. We have suggested that the method of plotting slices of the Q-symbol is desirable in this respect. An example was provided where the dynamics could be restricted to $SU(2)_{23}$, which

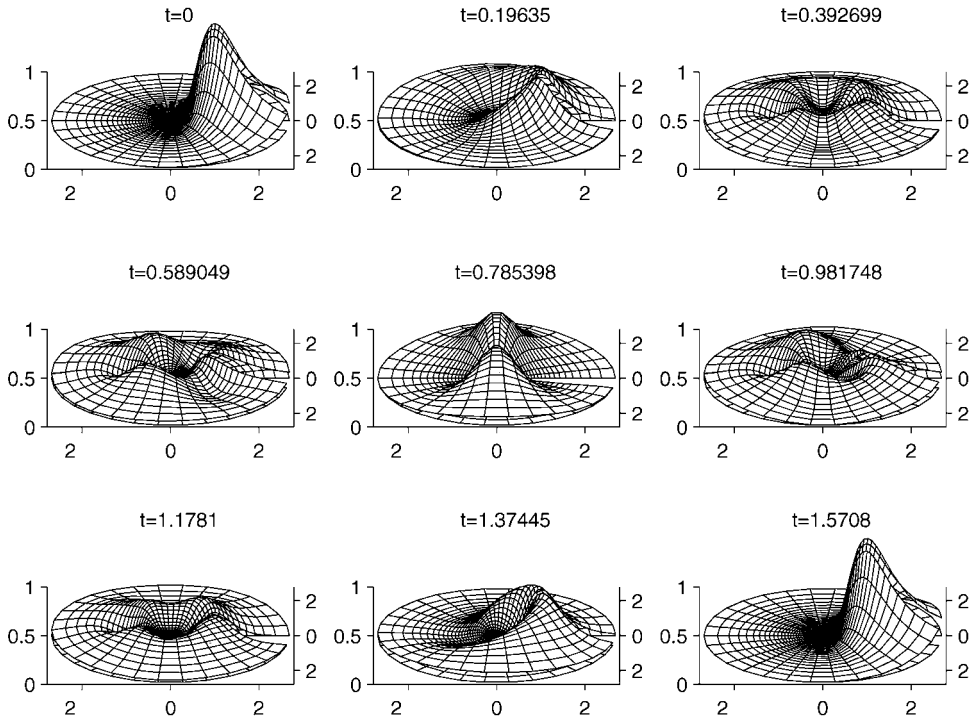

Figure 2. $\tilde{Q}(\xi, \phi_2)$ is plotted at a certain time t with the use of stereographical mapping. The origin corresponds to the north pole of the spherical subdomain (ξ, ϕ_2). Time flows from the top left figure at $t = 0$ to the bottom right figure at $t = \tau/2$. The recurrence time is a half of the even-number case in figure 1.

makes the plots quite clear and readily interpreted: a superposition of two $SU(2)$ coherent states is evident in these plots.

This approach may be extended to $SU(n)$ coherent states by generalizing the Hamiltonian (1) to n interacting modes. However, the $SU(3)$ dynamics is the most relevant case to current physical realizations. Although nonlinear optics and Bose–Einstein condensation have been specifically mentioned, any three-boson system with the given nonlinear evolution (1) could yield superpositions of $SU(3)$ coherent states, provided that the initial state is itself an $SU(3)$ coherent state.

Acknowledgments

KN would like to thank G J Milburn for useful discussions. KN acknowledges the financial support of the Australian International Education Foundation (AIEF). This paper has been supported by an Australian Research Council Large Grant and by a Macquarie University Research Grant.

References

[1] Yurke B and Stoler D 1986 *Phys. Rev. Lett.* **57** 13
[2] Bužek V and Knight P L 1995 *Prog. Opt.* **34** 1–158

[3] Milburn G J 1986 *Phys. Rev.* A **33** 13
[4] Sanders B C 1992 *Phys. Rev.* A **45** 6811
Sanders B C 1992 *Phys. Rev.* A **46** 2966 (erratum)
Chai C L 1992 *Phys. Rev.* A **46** 7187
Wielinga B and Sanders B C 1993 *J. Mod. Opt.* **40** 1923
Ansari N A and Man'ko V I 1994 *Phys. Rev.* A **50** 1942
[5] Perelomov A 1986 *Generalized Coherent States and Their Applications* (Berlin: Springer)
[6] Sanders B C 1989 *Phys. Rev.* A **40** 2417
[7] Gerry C C 1987 *Phys. Rev.* A **35** 2146
[8] Wang X-G, Sanders B C and Pan S-H 2000 *J. Phys. A: Math. Gen.* **33** 7451
[9] Radcliffe J M 1971 *J. Phys. A: Math. Gen.* **4** 313
[10] Arecchi F T, Courtens E, Gilmore R and Thomas H 1972 *Phys. Rev.* A **6** 2211
[11] Yurke B, McCall S L and Klauder J R 1986 *Phys. Rev.* A **33** 4033
[12] Nemoto K, Holmes C A, Milburn G J and Munro W J 2001 *Phys. Rev.* A **63** 013604
[13] Corney J F, Milburn G J and Zhang W 1999 *Phys. Rev.* A **59** 4630
[14] Bollinger J J, Itano W M, Wineland D J and Heinzen D J 1996 *Phys. Rev.* A **54** R4649
[15] Milburn G J, Corney J, Wright E M and Walls D F 1997 *Phys. Rev.* A **55** 4318
[16] Sackett C A, Stoof H T C and Hulet R G 1998 *Phys. Rev. Lett.* **80** 2031
[17] Cornish S L, Claussen N R, Roberts J L, Cornell E A and Wieman C E 2000 *Phys. Rev. Lett.* **85** 1795
[18] Gnutzmann S and Kuś M 2000 *J. Phys. A: Math. Gen.* **31** 9871
[19] Nemoto K 2000 *J. Phys. A: Math. Gen.* **33** 3493
[20] Rowe D J, Sanders B C and De Guise H 1999 *J. Math. Phys.* **40** 3604
[21] Gagen M J 1995 *Phys. Rev.* A **51** 2715